

Electronic Supplementary Information for:

Light harvesting enhancement upon incorporating alloy structured CdSe_XTe_{1-X} quantum dots in DPP:PC₆₁BM bulk heterojunction solar cell

Rezvan Soltani^a, Ali Asghar Katbab^a*, Kerstin Schaumberger^b, Nicola Gasparini^b, Christoph J. Brabec^{b,c}, Stefanie Rechberger^d, Erdmann Spiecker^d, Antoni Gimeno Alabau^e, Andres Ruland^f, Avishek Saha^g, Dirk M. Guldi^g, Vito Sgobba^c and Tayebeh Ameri^b**

^a Department of Polymer Engineering, Amirkabir University of technology, Tehran, 1591634311, Iran

^b Materials for Electronics and Energy Technology (i-MEET), Friedrich-Alexander-University Erlangen-Nuremberg, Martensstraße 7, 91058 Erlangen , Germany

^c ZAE - Bayerisches Zentrum für Angewandte Energieforschung e.V., Bavarian Center for Applied Energy Research, Haberstr. 2a, 91058 Erlangen

^d Institute of Micro- and Nanostructure Research & Center for Nanoanalysis and Electron Microscopy (CENEM), Friedrich-Alexander-University Erlangen-Nuremberg, Cauerstrasse 6, 91058 Erlangen, Germany

^e C/Teniente Mut nº58 p2, CP 46610 Guadassuar, Valencia, Spain

^f Intelligent Polymer Research Institute (IPRI), Innovation Campus, Squires Way, North Wollongong, NSW, 2500, Australia

^g Department of Chemistry and Pharmacy and Interdisciplinary Center for Molecular Materials (ICMM), Friedrich-Alexander-Universität Erlangen-Nürnberg, Egerlandstraße 3, 91058 Erlangen, Germany.

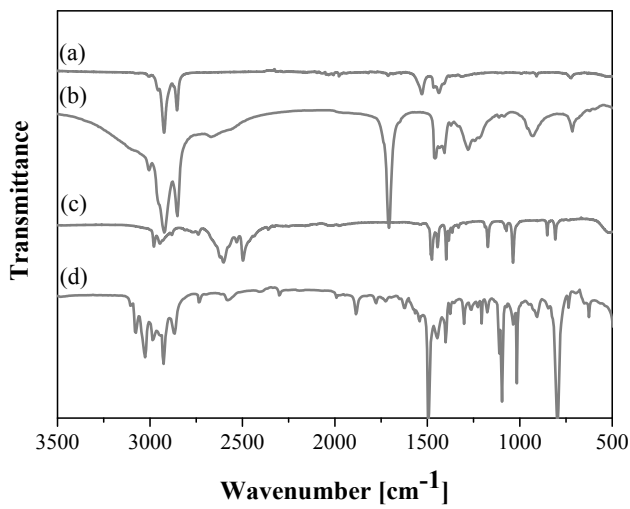


Figure S1. FT-IR spectra of (a) oleate capped CdSe_xTe_{1-x} QDs (before ligand exchange), (b) p-methylthiolate capped CdSe_xTe_{1-x} QDs (after ligand exchange), (c) oleic acid, and (d) p-methylthiophenole.

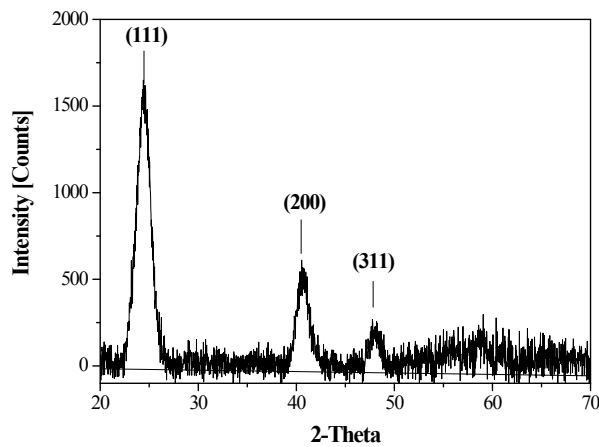


Figure S2. Powder x-ray diffractogramm of CdSe_xTe_{1-x} QDs demonstrating their cubic zinc blende crystallinity.

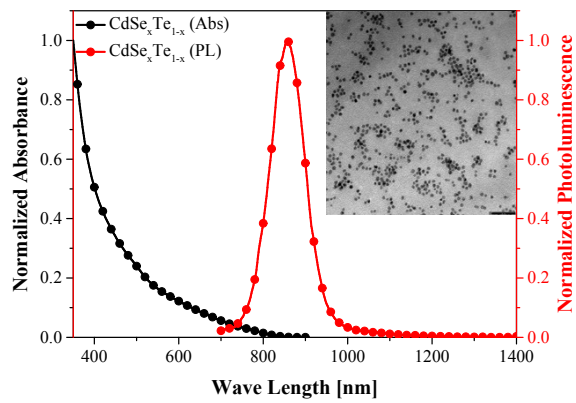


Figure S3. UV-Vis absorption and PL spectra of methylthiophenol-capped $\text{CdSe}_x\text{Te}_{1-x}$ nanoparticles. (Inset: TEM image of nanoparticles (the scale bar is 50 nm)).

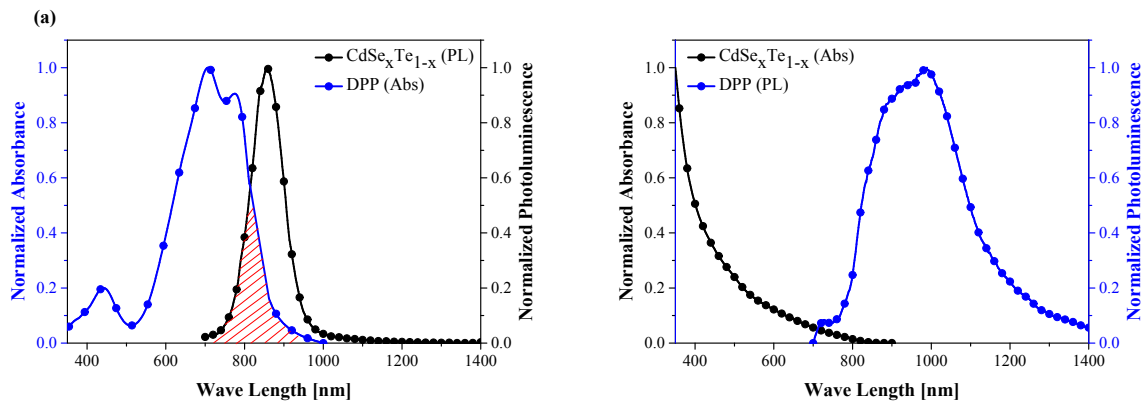


Figure S4. (a) UV-Vis absorption and PL spectra of DPP and $\text{CdSe}_x\text{Te}_{1-x}$ NPs respectively, (b) UV-Vis absorption and PL spectra of $\text{CdSe}_x\text{Te}_{1-x}$ NPs and DPP respectively.

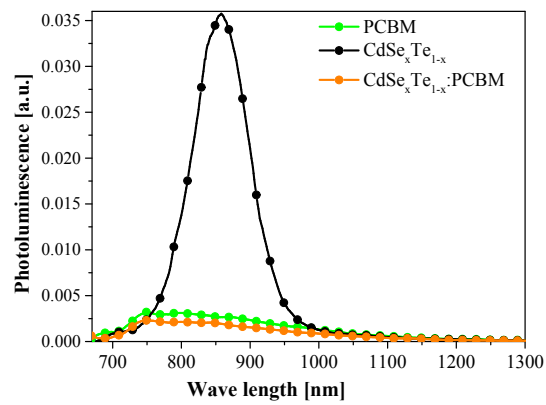


Figure S5. Photoluminescence spectra of PCBM, CdSe_xTe_{1-x} and CdSe_xTe_{1-x}:PCBM

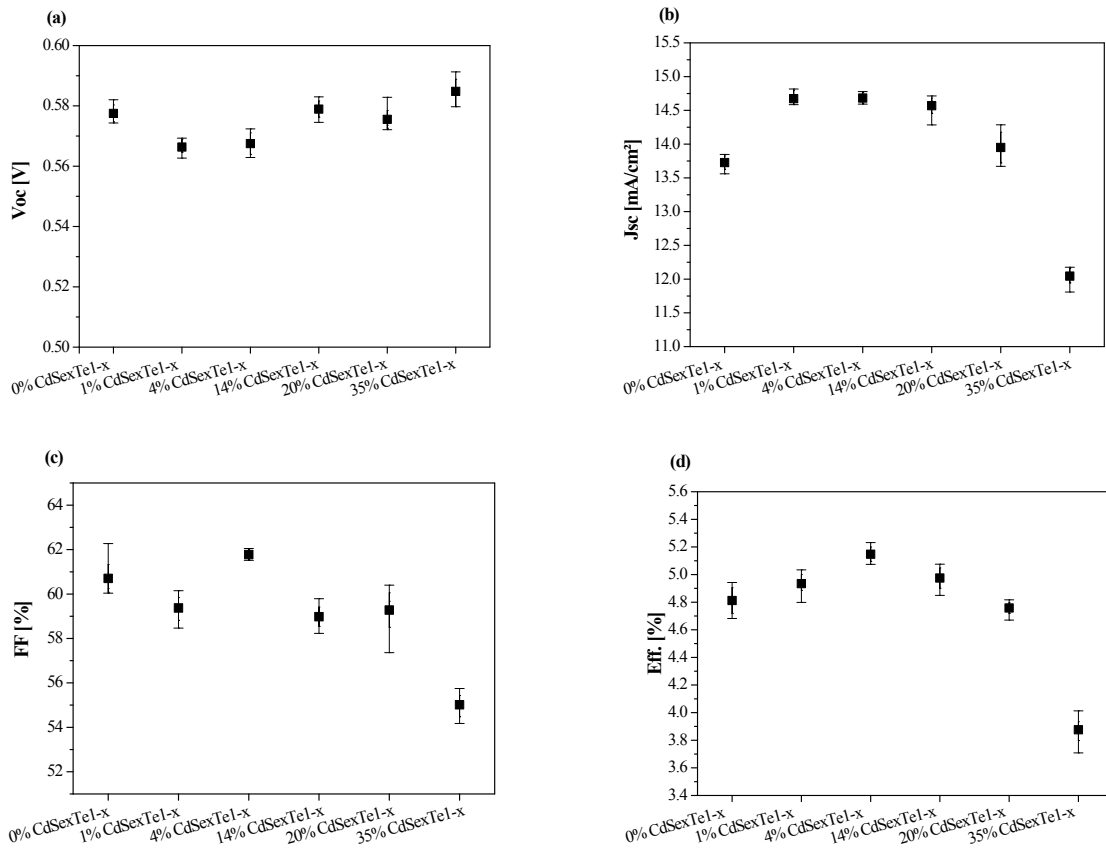


Figure S6. Box diagrams displaying (a) V_{oc} , (b) J_{sc} , (c) FF and (d) PCE of 6 cells containing different CdSe_xTe_{1-x} content.

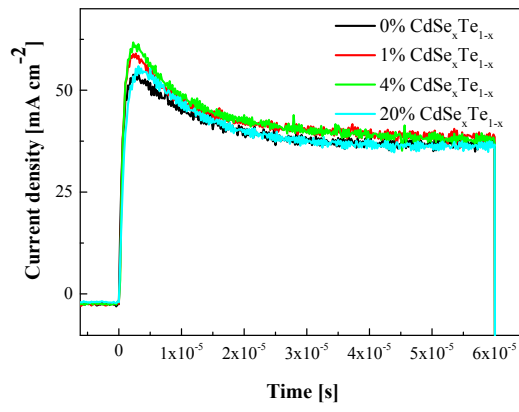


Figure S7. Time dependent photo-CELIV traces of hybrid solar cells with different $\text{CdSe}_x\text{Te}_{1-x}$ concentrations.

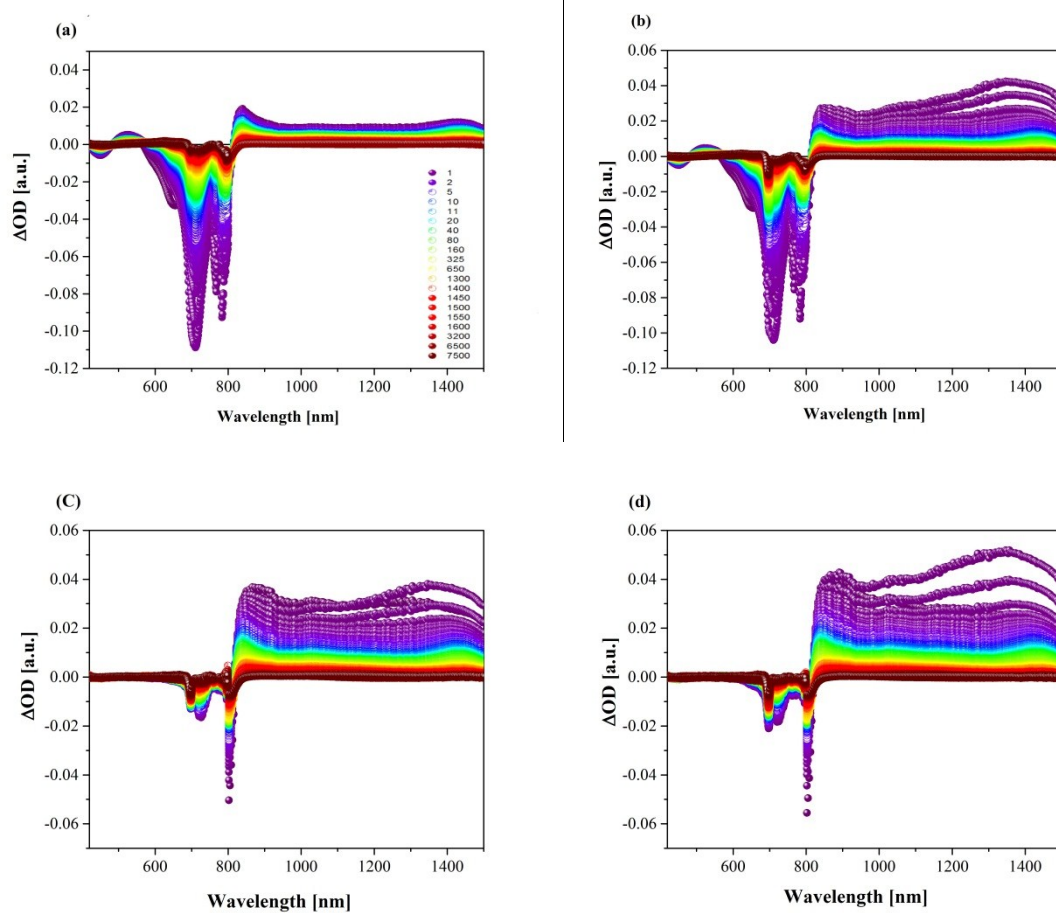


Figure S8. Differential absorption spectra upon excitation at 695 nm (100 nJ) of ternary film containing (a) 1 wt.% $\text{CdSe}_x\text{Te}_{1-X}$, (b) 4 wt.% $\text{CdSe}_x\text{Te}_{1-X}$, (c) 14 wt.% $\text{CdSe}_x\text{Te}_{1-X}$, and (d) 20 wt.% $\text{CdSe}_x\text{Te}_{1-X}$. The numbers reported in the legend correspond to the time delays in ps.